The primary extinction approach considered can be used for the analysis of the diffraction data, measured on polycrystals, if the dislocation density in a crystal grain satisfies the applicability condition of the mosaic model.

We would like to thank the referees for their helpful suggestions for improvements to the paper.

References

AIKALA, O. & MANSIKKA, K. (1972). *Phys. Kondens. Mater.* **14**, 105–110.

BECKER, P. (1977). *Acta Cryst.* A**33**, 243–249.

BECKER, P. J. & COPPENS, P. (1974*a*). *Acta Cryst.* A**30**, 129–147.

BECKER, P. & COPPENS, P. (1974*b*). *Acta Cryst.* A**30**, 148–153.

BECKER, P. & COPPENS, P. (1975). *Acta Cryst.* A**31**, 417–425.

COOPER, M. J. (1979). *Acta Cryst.* A**35**, 176–180.

COOPER, M. J. & ROUSE, K. D. (1970). *Acta Cryst.* A**26**, 214–223.

COOPER, M. J. & ROUSE, K. D. (1976). *Acta Cryst.* A**32**, 806–812.

COPPENS, P. & HAMILTON, W. C. (1970). *Acta Cryst.* A**26**, 71–83.

CROMER, D. T. & LIBERMAN, D. (1970). *J. Chem. Phys.* **53**, 1891–1898.

DARWIN, C. C. (1914). *Philos. Mag.* **27**, 315–340.

DENNE, W. A. (1972). *Acta Cryst.* A**28**, 192–201.

HOWARD, C. J. & JONES, R. D. G. (1977). *Acta Cryst.* A**33**, 776–783.

KATO, N. (1976). *Acta Cryst.* A**32**, 453–466.

KILLEAN, R. C. G., LAWRENCE, J. L. & SHARMA, V. C. (1972). *Acta Cryst.* A**28**, 405–407.

LAWRENCE, J. L. (1972). *Acta Cryst.* A**28**, 400–404.

LAWRENCE, J. L. (1973). *Acta Cryst.* A**29**, 208–210.

LAWRENCE, J. L. (1974). *Acta Cryst.* A**30**, 454–455.

LAWRENCE, J. L. (1977). *Acta Cryst.* A**33**, 232–234.

MATHIESON, A. MCL., CALVERT, L. D. & KILLEAN, R. C. G. (1974). *Annual Report* (1973–1974), pp. 24–26. Division of Chemical Physics, CSIRO, Clayton, Australia.

MICHELL, D., SMITH, A. P. & SABINE, T. M. (1969). *Acta Cryst.* B**25**, 2458–2460.

OLEKHNOVICH, N. M. (1978). *Dokl. Akad. Nauk B. SSR*, **22**, 506–509.

OLEKHNOVICH, N. M., KARPEI, A. L. & MARKOVICH, V. L. (1978). *Krist. Tech.* **13**, 1463–1469.

OLEKHNOVICH, N. M. & MARKOVICH, V. L. (1978). *Kristallografiya*, **23**, 658–661.

OLEKHNOVICH, N. M. & OLEKHNOVICH, A. I. (1978). *Acta Cryst.* A**34**, 321–326.

OLEKHNOVICH, N. M. & OLEKHNOVICH, A. I. (1980). *Acta Cryst.* A**36**, 22–27.

OLEKHNOVICH, N. M., RUBCOV, V. A. & SCHMIDT, M. P. (1975). *Kristallografiya*, **20**, 796–802.

OLEKHNOVICH, N. M. & SCHMIDT, M. P. (1977). *Isv. Akad. Nauk B. SSR, Fiz. Mat. Nauk*, **1**, 118–122.

SHARMA, V. C. (1974). *Acta Cryst.* A**30**, 278–280.

TAKAGI, S. (1969). *J. Phys. Soc. Jpn*, **26**, 1239–1253.

WERNER, A. S. (1969). *Acta Cryst.* A**25**, 639.

ZACHARIASEN, W. H. (1967). *Acta Cryst.* **23**, 558–564.

ZACHARIASEN, W. H. (1968*a*). *Acta Cryst.* A**24**, 212–216.

ZACHARIASEN, W. H. (1968*b*). *Acta Cryst.* A**24**, 324–325.

Acta Cryst. (1980). A**36**, 996–1001

Anomalous Dispersion of Small-Angle Scattering of Horse-Spleen Ferritin at the Iron *K* Absorption Edge

BY H. B. STUHRMANN

European Molecular Biology Laboratory, EMBL Outstation at DESY, Notkestrasse 85, *D*-2000 *Hamburg* 52, *Federal Republic of Germany*

(*Received* 6 *May* 1980; *accepted* 7 *July* 1980)

Abstract

Small-angle scattering experiments of horse-spleen ferritin solutions have been performed at various wavelengths near the *K* absorption edge of iron, using synchrotron radiation from the storage ring DORIS. The anomalous dispersion of the atomic form factor f as described by f' and if'' has been monitored by the dependence of the radius of gyration R and the absorption coefficient μ respectively. There is a 4% increase of R at the absorption edge. The relative full half width of this peak of 0·0016 corresponding to 11 eV of the energy scale reflects the drastic variation of f' by 7 electrons. The predictable relation between R and μ has been verified by the Kramers–Kronig relation. As small-angle scattering is primarily influenced by f', best

0567-7394/80/060996-06$01.00

advantage from anomalous dispersion in small-angle scattering can be taken by measurements very near the absorption edges.

Introduction

The selective change of the scattering density is one of the most fruitful methods in structure determination. As small-angle scattering is a low-resolution technique, the markers have to be rather big in order to provide a measurable excess scattering intensity of macromolecules in solution. It is for this reason that isotopic replacement methods in neutron small-angle scattering have found wide application. The marker may either be introduced as a deuterated subunit in a more complex macromolecule or it may be defined by the excluded volume of the solute particle itself (Stuhrmann & Miller, 1978). Isotopic replacement hardly changes the structural properties of macromolecules and therefore may be regarded as a fairly reliable isomorphous replacement (Eisenberg & Cohen, 1968).

There are still better ways of introducing local changes of the scattering density in a macromolecule, which do not start from chemical or isotopic exchange procedures. At certain energies the scattering factor may change considerably because of electronic or nuclear excitations. Not only does the modulus of the form factor change, but there is also a variation of the phase difference between the incident and the scattered wave. Usually the anomalous dispersion of the scattering factor is taken into account by

$$f = f_0 + f' + if'' \tag{1}$$

(see for instance Rameseshan & Abrahams, 1974). ($f_0 + f'$) and f'' are the real and imaginary parts of the atomic form factor. f' and f'' contribute significantly to the atomic form factor near the electronic or nuclear resonance, whereas f_0 is observed in the off-resonance region.

Before entering into any detailed description of an experiment, an outline of the influence of anomalous dispersion on small-angle scattering will be given.

Anomalous dispersion and small-angle scattering

Let the excess scattering density of dissolved particles with respect to the density of the solvent be

$$\rho(\mathbf{r}) = \rho(\mathbf{r})_{\text{solute}} - \rho_{\text{solvent}}. \tag{2}$$

Similarly, (2) holds for the mean scattering densities:

$$\bar{\rho} = \bar{\rho}_{\text{solute}} - \rho_{\text{solvent}} \equiv \text{contrast}. \tag{2a}$$

Following the notation of the contrast variation we distinguish between the internal structure $\rho_s(\mathbf{r})$ observed at vanishing contrast and the shape of the macromolecular volume excluded to solvent molecules $\rho_c(\mathbf{r})$ (Stuhrmann & Kirste, 1965).

$$\rho(\mathbf{r}) = \bar{\rho}\,\rho_c(\mathbf{r}) + \rho_s(\mathbf{r}). \tag{3}$$

Inside the volume $\rho_c(\mathbf{r})$ there may be regions defined by $\rho_a(\mathbf{r})$, where anomalous scatterers add to the scattering density

$$\rho(\mathbf{r}) = \rho_s(\mathbf{r}) + \bar{\rho}\,\rho_c(\mathbf{r}) + (\bar{\rho}' + i\bar{\rho}'')\,\rho_a(\mathbf{r}), \tag{4}$$

$\bar{\rho}'$ and $\bar{\rho}''$ are the anomalous scattering densities in $\rho_a(\mathbf{r})$. $\rho_a(\mathbf{r})$ may be restricted to the sites of very few metal atoms (*e.g.* in metal enzymes) or it may contain numerous heavy atoms (*e.g.* mineral FeOOH micelle in ferritin). Finally, the solute free of anomalous scatterers may be embedded in a solvent with complex scattering density. In this case the boundaries of $\rho_a(\mathbf{r})$ coincide with the shape $\rho_c(\mathbf{r})$:

$$\rho(\mathbf{r}) = \rho_s(\mathbf{r}) + (\bar{\rho} + \bar{\rho}' + i\bar{\rho}'')\,\rho_c(\mathbf{r}). \tag{5}$$

Starting from the more general equation (4), small-angle scattering $I(h)$ will depend on the contrast as described by the following equation:

$$I(h) = (\bar{\rho}'^2 + \bar{\rho}''^2)\,I_a(h) + \bar{\rho}'[\bar{\rho}I_{ac}(h) + I_{as}(h)] + \bar{\rho}^2 I_c(h) + \bar{\rho}I_{cs}(h) + I_s(h). \tag{6}$$

The basic scattering functions I_c, I_{cs} and I_s of the classical contrast variation would be left, if (3) had been used (Stuhrmann & Kirste, 1965). The anomalous scatterers in $\rho_a(\mathbf{r})$ give rise to the scattering functions $I_a(h)$, $I_{ac}(h)$ and $I_{as}(h)$. As examples, a pure term and a cross term are given in detail:

$$I_a(h) = \int\int \rho_a(\mathbf{r})\,\rho_a(\mathbf{r}')\,\frac{\sin h|\mathbf{r}-\mathbf{r}'|}{h|\mathbf{r}-\mathbf{r}'|}\,\mathrm{d}^3r\,\mathrm{d}^3r'$$

and

$$I_{ac}(h) = 2\int\int \rho_a(\mathbf{r})\,\rho_c(\mathbf{r}')\,\frac{\sin h|\mathbf{r}-\mathbf{r}'|}{h|\mathbf{r}-\mathbf{r}'|}\,\mathrm{d}^3r\,\mathrm{d}^3r'.$$

I_c, I_s, I_{cs} and I_{as} are written correspondingly. The cross terms I_{ac} and I_{as} are due to convolutions of $\rho_a(\mathbf{r})$ with $\rho_c(\mathbf{r})$ and $\rho_s(\mathbf{r})$ respectively. By variation of $\bar{\rho}$, $\bar{\rho}'$ and $\bar{\rho}''$ six characteristic functions I_a, I_{ac}, I_{as}, I_c, I_{cs} and I_s can be determined. This method is called complex contrast variation (CCV). A method for the independent determination of $\bar{\rho}'$ and $\bar{\rho}''$ will be given below.

If there is no anomalous scattering, (6) reduces to its classical form with I_c, I_{cs} and I_s as characteristic functions (Stuhrmann & Kirste, 1965):

$$I(h) = \bar{\rho}^2 I_c(h) + \bar{\rho}\,I_{cs}(h) + I_s(h). \tag{7}$$

A similar formula results if $\rho_a(\mathbf{r}) = \rho_c(\mathbf{r})$ (Stuhrmann, 1976):

$$I(h) = [(\bar{\rho} + \bar{\rho}')^2 + \bar{\rho}''^2]I_c(h) + (\bar{\rho} + \bar{\rho}')I_{cs}(h) + I_s(h). \tag{8}$$

Contrast variation in a solvent with complex scattering density yields the same characteristic scattering functions as real contrast variation.

The dependence of the radius of gyration on the complex contrast

Among the parameters of $\rho(\mathbf{r})$ determined from small-angle scattering, the squared radius of gyration

$$R^2 = \frac{1}{2} \frac{\int\int \rho(\mathbf{r})\,\rho(\mathbf{r}')\,|\mathbf{r}-\mathbf{r}'|^2\,\mathrm{d}^3r\,\mathrm{d}^3r'}{\int\int \rho(\mathbf{r})\,\rho(\mathbf{r}')\,\mathrm{d}^3r\,\mathrm{d}^3r'} \qquad (9)$$

is most easily accessible. From the initial slope of a scattering curve represented in a Guinier plot [$\log I(h)$ *versus* h^2], R is readily calculated. In order to derive the dependence of the radius of gyration on the complex contrast the sine function in (6) is developed as a power series, and the term in h^2 is compared with the definition of R in (9):

$$\begin{aligned} R^2 = [&\bar{\rho}^2 V_c m_c + (\bar{\rho}'^2 + \bar{\rho}''^2)(V_a m_a - \mathbf{n}_a.\mathbf{n}_a) \\ &+ \bar{\rho}\bar{\rho}'(V_a m_c + V_c m_a) \\ &+ \bar{\rho} V_c m_s + \bar{\rho}'(V_a m_s - 2\mathbf{n}_s.\mathbf{n}_a) - \mathbf{n}_s.\mathbf{n}_s] \\ &\times [(\bar{\rho}V_c - \bar{\rho}V_a)^2 + \bar{\rho}''^2 V_a^2]^{-1}, \end{aligned} \qquad (10)$$

where

$$V_a = \int \rho_a(\mathbf{r})\,\mathrm{d}^3r,$$

$$m_a = \int \rho_a(\mathbf{r})\,r^2\,\mathrm{d}^3r$$

and

$$\mathbf{n}_a = \int \rho_a(\mathbf{r})\,\mathbf{r}\,\mathrm{d}^3r.$$

V_c, m_c and $\mathbf{n}_c$ are defined similarly to V_a, m_a and $\mathbf{n}_a$. It has been assumed that the center of mass of $\rho_c(\mathbf{r})$ is at the origin. If there are no anomalous scatterers (10) simplifies to

$$\begin{aligned} R^2 &= [\bar{\rho}^2 V_c m_c + \bar{\rho} V_c m_s - \mathbf{n}_s.\mathbf{n}_s)/(\bar{\rho}^2 V_c^2) \\ &= m_c/V_c + m_s/(\bar{\rho}V_c) - \mathbf{n}_s.\mathbf{n}_s/(\bar{\rho}V_c)^2 \\ &\equiv R_c^2 + \alpha/\bar{\rho} - \beta/\bar{\rho}^2. \end{aligned} \qquad (11)$$

This is the dependence of R on $\bar{\rho}$ in real contrast variation (Stuhrmann, Tardieu, Mateu, Sardet, Luzzati, Aggerbeck & Scanu, 1975). The same coefficients R_c, α and β can be determined if anomalous scatterers are in the solvent only:

$$R^2 = R_c^2 + \alpha \frac{\bar{\rho} + \bar{\rho}'}{(\bar{\rho} + \bar{\rho}')^2 + \bar{\rho}''^2} - \beta \frac{1}{(\bar{\rho} + \bar{\rho}')^2 + \bar{\rho}''^2}. \qquad (12)$$

Another interesting case is given by spherical structures, which contain anomalous scatterers in one or a few shells only. As this model will be used to analyze the dependence of the radius of gyration of ferritin on the wavelength, the relation between R and f' (f'') is discussed here.

Starting from (10), all contributions from non-spherical parameters have to be dropped first.

$$\begin{aligned} R^2 = [&\bar{\rho}^2 V_c m_c + (\bar{\rho}'^2 + \bar{\rho}''^2) V_a m_a \\ &+ \bar{\rho}\bar{\rho}'(V_a m_c + V_c m_a) + \bar{\rho} V_c m_s \\ &+ \bar{\rho}' V_a m_s]/[(\bar{\rho}V_c + \bar{\rho}'V_a)^2 + \bar{\rho}''^2 V_a^2]. \end{aligned} \qquad (13)$$

If $\bar{\rho}'$, $\bar{\rho}'' \ll \bar{\rho}$ then this equation can be reduced to the following relationship between the relative change of $\Delta R^2/R^2$ and the increase of the scattering density by $\Delta\bar{\rho}'$:

$$\frac{\Delta R^2}{R^2} = \left(\frac{R_a^2}{R^2} - 1\right) \frac{V_a}{V_c} \frac{\Delta\bar{\rho}'}{\bar{\rho}}. \qquad (14)$$

$\Delta\bar{\rho}'\,V_a$ is the number of 'anomalous electrons' due to f', and $\bar{\rho}V_c$ is the total number of excess electrons of the solute with respect to the solvent.

Experimental

Small-angle scattering of horse-spleen ferritin has been measured at wavelengths near the K absorption edge of iron (λ_K = 1·743 Å) using synchrotron radiation from the storage ring DORIS of the Deutsches Eletronen-synchrotron (DESY) at Hamburg (Stuhrmann, 1978). The 10% ferritin solutions (from E. Merck, Darmstadt) were either used as such or diluted to a concentration of 3·5%. Most of the data presented here have been obtained from 3·5% solutions. The sample thickness was 1·5 mm.

Small-angle scattering experiments were carried out at the instrument X15 of the European Molecular Biology Laboratory at DESY Hamburg. A description of the instrument is being prepared. Therefore, only some characteristic elements of the instrument will be given here.

X-ray synchrotron radiation filtered by 0·6 mm Be hits a Ge single crystal of 25 mm width, 75 mm length and 1 mm thickness at 23 m from the source. Monochromatic radiation from the asymmetric cut of the Ge crystal ($\alpha = 7°$) emerges in the vertical plane. A second Ge crystal at 1·22 m above the white-beam direction deflects the monochromatic beam into the horizontal plane and further to the small-angle instrument. The faces of both crystals are parallel and they are mounted in such a way that the beam is expanded by the first crystal and compressed by the second crystal (Kohra, Ando, Matsuhita & Hashizume, 1978).

The distances between the two crystals may vary between 1·7 and 3·5 m. This restriction is mainly due to the extreme lengths of the telescope tubes ensuring a vacuum path between the two monochromators and between the second monochromator and the stationary small-angle camera. Therefore, the angles of beam deflection 2θ may vary between 22 and 47°. This corresponds to wavelengths from 1·25 to 2·60 Å, using the Ge 111 reflection. Higher-order harmonics are ignored by the position-sensitive Ar-filled proportional counter.

The small-angle instrument consists of three sections of steel tubes of 150, 250 and 350 mm diameter respectively. It has a total length of about 8 m. A position-sensitive area detector is mounted at the end of the instrument. The sensitive area is 200 × 200 mm and the resolution is determined by the wire spacing of 2 mm.

The distance between the sample and the detector can be varied in discrete steps of a geometrical series from 7·2 m down to 0·36 m (Fig. 1). A distance of 3·6 m has been chosen for the small-angle experiments with ferritin solutions.

The solutions were kept in a temperature-controlled Mark capillary of 1·5 mm diameter. About 10 mm horizontal length and 1 mm height of the capillary were irradiated. The absorption of the ferritin solution was measured as the ratio of the currents of two ionization chambers in front of and closely behind the sample. At each chosen wavelength small-angle scatter was measured for five minutes. The count-rates of the detector were around 20 000 counts s^{-1}.

Results and discussion

Ferritin is an iron-storing protein. Its 24 subunits form a hollow sphere of 120 Å outer and 74 Å inner diameter (Harrison, 1963; Fishbach & Anderegg, 1965; Bielig, Kratky, Rohns & Haward, 1966; Stuhrmann, Haas, Ibel, Koch & Crichton, 1976). The iron-free ferritin has a molecular weight of 440 000 (Crichton, 1973; Bielig *et al.*, 1966; Harrison, 1963). The core of the apoferritin molecule is filled with variable amounts of ferric iron mostly as FeOOH, but with 1 to 1·5% phosphate (Laufberger, 1947). Saturated ferritin from horse spleen may contain up to 4300 iron atoms, which nearly doubles its molecular weight (Fishbach & Anderegg, 1965; Harrison, 1963).

The exceptional chemical composition and structure make ferritin an extremely suitable candidate for a first study of anomalous dispersion in small-angle scattering. Therefore, the most typical parameter of small-angle scattering, the radius of gyration, was measured at some ten wavelengths near the K absorption edge of iron. There is practically no variation of R except at the absorption edge, where it increases by about 4% to a sharp peak with a full half width of 0·0026 Å or 11 eV on the energy scale (Fig. 2).

It has been shown in (14) that the increase of R is proportional to the increase of the negative f'. As the difference in R is rather small, we may rewrite (14):

$$\frac{\Delta R}{R} = \frac{1}{2}\left(\frac{R_a^2}{R^2} - 1\right) \times \frac{\text{number of anomalous electrons}}{\text{number of all excess electrons}}. \qquad (15)$$

In the off-resonance region the mean radius of gyration of the dissolved ferritin molecules is 42 Å. This value lies well between those of iron-free apoferritin (51·5 Å) and of 'full' ferritin (38 Å) (Fishbach & Anderegg, 1965). As saturated ferritin contains about 4300 iron atoms, an average iron content of about 3000 iron atoms is estimated for the present ferritin sample (Stuhrmann & Duée, 1975). From (15) and with reference to the radius of gyration of the FeOOH core, R_a = 28 Å (Fishbach & Anderegg, 1965), the relative increase of R at the K absorption edge indicates 14% decrease of the contrast of ferritin, due to the anomalous dispersion of iron.

The scattering density of the core decreases by as much as 17% and the atomic form factor of iron changes its value by one quarter (7 electrons in f').

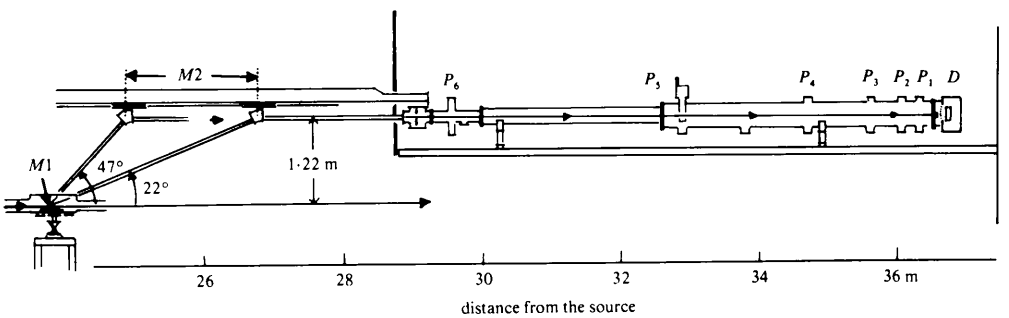

Fig. 1. Small-angle instrument X15 of the EMBL Outstation at DESY, Hamburg. Synchrotron radiation from the storage ring DORIS is deflected by the crystal monochromators $M1$ and $M2$. The scatter is recorded by a two-dimensional position-sensitive counter (D); $P1$ to $P6$ are possible sample positions.

What about the absolute value of f'? The question cannot be answered on the basis of the data presented here. The relative variation of the wavelength is only 2%! However, from the comparison with other experiments and theoretical considerations one can assume a maximum peak height of f' of 11 electrons (Freund, 1974).

Near the K absorption edge the absorption coefficient μ (in mm^{-1} at mass density = 1 Mg/m^3) is

$$\mu = \frac{2N_L}{A}\lambda\frac{e^2}{mc^2}f'' = \frac{337{\cdot}1}{A}\lambda f'', \qquad (16)$$

$N_L = 6{\cdot}02 \times 10^{23}$, A = atomic weight, e^2/mc^2 = Thomson scattering factor = $2{\cdot}8 \times 10^{-12}$ mm, λ = wavelength in Å. The maximum change of the extinction by $(0{\cdot}07 \pm 0{\cdot}01)$ mm^{-1} of the 3·5% ferritin solution results in an absorption coefficient difference of (60 ± 10) mm^{-1}. The imaginary part f'' of the atomic factor of iron in the mineral FeOOH core of ferritin varies by $(5{\cdot}7 \pm 1)$ electrons.

In a small energy range f'' is proportional to μ. The extinction of a 3·5% ferritin solution is given in Fig. 3. It shows strong oscillations at the short-wavelength side of the absorption edge, which have been analyzed by Heald, Stern, Bunker, Holt & Holt (1979). In order to establish the consistence of μ with R, we make use of the Kramers–Kronig relation between f' and f''

$$f'(\omega) = \frac{2}{\pi}\int \frac{\omega' f''(\omega')\,d\omega'}{\omega^2 - \omega'^2}, \qquad (17)$$

$$\omega = 2\pi c/\lambda.$$

As this study is aiming at the dispersion of f' and f'' near the absorption edge only, (17) can be simplified,

$$f'(\omega) = -\frac{1}{\pi}\int_{\varepsilon=-\delta}^{\varepsilon=\delta} \frac{f''(\omega+\varepsilon)}{\varepsilon}\,d\varepsilon, \qquad (17a)$$

where δ is of the order of 0·01.

As R and μ are related to f' and f'' respectively, the application of the Kramers–Kronig relation provides a test of the previous assumptions:

The absorption coefficient μ yields f'' using (16), f'' is connected with f' by the Kramers–Kronig relation (equation 17), and from f' the anomalous dispersion of R of ferritin is calculated (equation 14). Fig. 2 shows that there is satisfactory agreement between anomalous dispersion of R as directly determined from small-angle scattering and R as derived from the absorption spectrum.

The relation between f' and f'' is best illustrated as in Fig. 4, which shows the measured pairs of f' and f'' on a nearly circular line. The average diameter of the circle is 7 electrons, as has already been deduced from the analysis of R. Near the absorption edge the anomalous dispersion of f' and f'' behaves as if it were due to a single resonance.

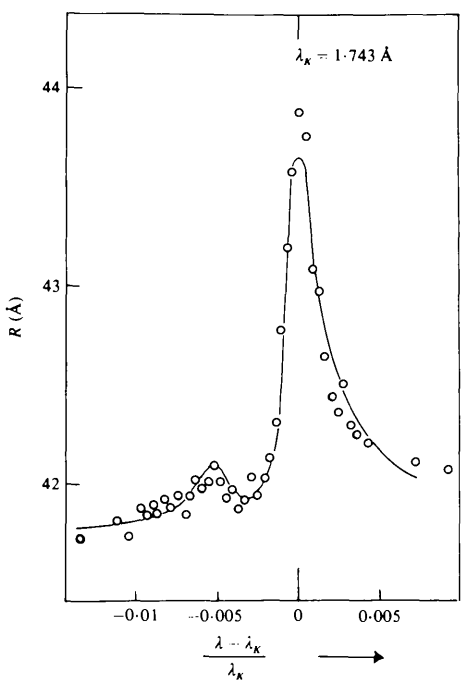

Fig. 2. The dependence of the apparent radius of gyration, R(○), of ferritin on the wavelength near the K absorption edge. —— R as calculated from the absorption spectrum using the Kramers–Kronig relation. The fine structure of the absorption spectrum in Fig. 3 is clearly reflected in the behavior of R.

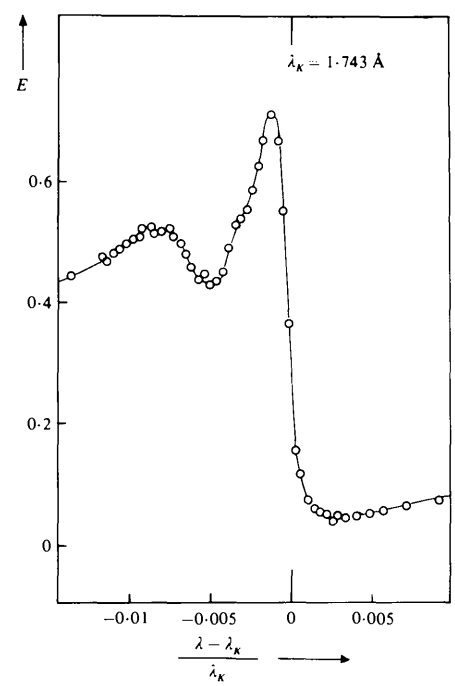

Fig. 3. The extinction $E = \mu x$ (x = sample thickness) of a 3·5% ferritin solution near the iron K absorption edge. x = 1·5 mm.

Conclusions

The use of anomalous dispersion in small-angle scattering of solutions relies mainly on the influence of f'. This is due to the well known fact that in the reciprocal space f' always adds to f in a constructive way, whereas terms linear in f'' will average out in small-angle scattering. The squares of f' and f'' are conserved.

A strong variation of f' as a function of the wavelength is observed only at the absorption edge. Therefore, small-angle scattering experiments need to be carried out over a small, relative wavelength range of less than 1% only. A good energy resolution, as is achieved with a single crystal, is essential.

Future applications of anomalous dispersion in small-angle scattering will start from solvents with anomalous scattering densities. Small-angle scattering of proteins in 30% rubidium bromide solutions would nearly match the electron density of the solute. The influence of the anomalous scattering factors of Rb and Br at the K absorption edges at 0·8 and 0·9 Å respectively would be greatly enhanced and allow the determination of the characteristic functions of contrast variation.

The L edge of cesium at $\lambda = 2{\cdot}4$ Å is an even more powerful tool for the variation of f' (Phillips, Templeton, Templeton & Hodgson, 1978). The determination of the geometrical arrangement of metal atoms in enzymes might be a more rewarding project. It must, however, be emphasized that a considerable increase in the accuracy of the presently available small-angle data will have to be achieved.

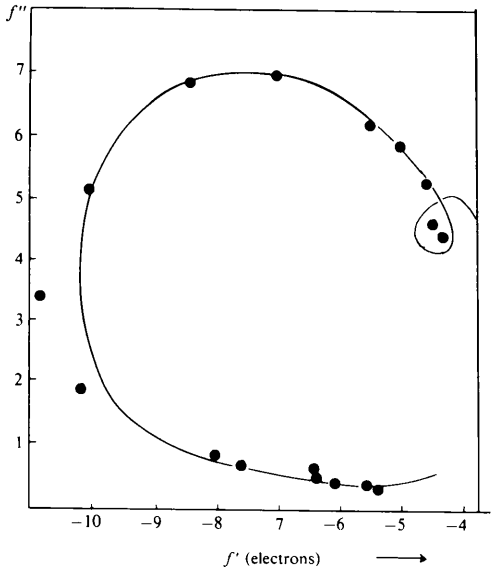

Fig. 4. The relation between f' and f'' at the K absorption edge of iron in the FeOOH micelle of ferritin. The dots (•) are derived from the measured R and μ. —— f' calculated from f'' using the Kramers–Kronig relation. The loop is a consequence of the Kronig oscillations of f' and f''.

References

BIELIG, H. J., KRATKY, O., ROHNS, G. & HAWARD, H. (1966). *Biochim. Biophys. Acta*, **112**, 110–118.

CRICHTON, R. R. (1973). *Struct. Bonding (Berlin)*, **17**, 67–134.

EISENBERG, H. & COHEN, G. (1968). *J. Mol. Biol.* **37**, 355–362; *erratum: J. Mol. Biol.* (1968), **42**, 607.

FISHBACH, F. A. & ANDEREGG, J. W. (1965). *J. Mol. Biol.* **14**, 458–473.

FREUND, A. (1974). *Anomalous Scattering*, edited by S. RAMESESHAN & S. C. ABRAHAMS, pp. 69–83. Copenhagen: Munksgaard.

HARRISON, P. M. (1963). *J. Mol. Biol.* **6**, 404–422.

HEALD, S. M., STERN, E. A., BUNKER, B., HOLT, E. M. & HOLT, S. L. (1979). *J. Am. Chem. Soc.* **101**, 67–72.

KOHRA, K., ANDO, M., MATSUHITA, T. & HASHIZUME, H. (1978). *Synchrotron Radiation, Instrumentation and Developments*, edited by F. WUILLEUMIER & Y. FARGE, pp. 161–166. Amsterdam: North-Holland.

LAUFBERGER, V. (1947). *Bull. Soc. Chem. Biol.* **79**, 1575–1582.

PHILLIPS, J. C., TEMPLETON, D. H., TEMPLETON, L. K. & HODGSON, K. O. (1978). *Science*, **201**, 257–259.

RAMESESHAN, S. & ABRAHAMS, S. C. (1974). *Anomalous Scattering*. Copenhagen: Munksgaard.

STUHRMANN, H. B. (1976). *Brookhaven Symp. Biol.* **27**, IV 3–19.

STUHRMANN, H. B. (1978). *Prog. Biophys.* **11**, 71–98.

STUHRMANN, H. B. & DUÉE, E. (1975). *J. Appl. Cryst.* **8**, 538–542.

STUHRMANN, H. B., HAAS, J., IBEL, K., KOCH, M. H. J. & CRICHTON, R. R. (1976). *J. Mol. Biol.* **100**, 399–413.

STUHRMANN, H. B. & KIRSTE, R. G. (1965). *Z. Phys. Chem. (Frankfurt)*, **46**, 247–250.

STUHRMANN, H. B. & MILLER, A. (1978). *J. Appl. Cryst.* **11**, 325–345.

STUHRMANN, H. B., TARDIEU, A., MATEU, L., SARDET, C., LUZZATI, V., AGGERBECK, L. & SCANU, A. M. (1975). *Proc. Natl Acad. Sci. USA*, **72**, 2270–2273.